

Lasers in Manufacturing Conference 2023

X-ray imaging of the influence of static and dynamic beam shaping on pore formation during laser welding of copper hairpins

Eveline N. Reinheimer^{a,*}, Christian Hagenlocher^a, Rudolf Weber^a, Thomas Graf^a

^aUniversität Stuttgart Institut für Strahlwerkzeuge, Pfaffenwaldring 43, 70569 Stuttgart, Germany

Abstract

Laser beam welding provides a very efficient process for joining copper pins in electric drives, which are referred to as hairpins. The occurrence of pores in such joints reduces the conducting cross-section area and increases the electric resistance. The present work is an investigation of the process pore and spatter formation during welding hairpins with different welding contours. The welds are observed by radiographing the capillary in the processing zone. With the observation it was possible to determine the influence of different contours on the formation of pores and spatters. The results show an influence of the welding contour on the formation of process pores and spatters. The occurrence of pores therefore influences the tensile strength of the welded hairpins.

Keywords: X-Ray Imaging; Copper; Hairpin Welding; Beam Shaping

1. Introduction

Laser beam welding is a very efficient process for joining copper hairpin windings in electric drives, which are referred to as hairpins. Pore formation and avoidance strategies in copper for linear welds were investigated by Alter et al., 2020; Heider et al., 2011; Heider, 2018. Glaessel et al., 2017 showed the capability of infrared lasers for welding hairpins and Bocksrocker et al. investigated the pore formation for a hairpin weld without a gap. Omlor et al. showed that process pores occur especially at the location of the gap between the two pins. The occurrence of pores reduces the conducting cross-sectional area, which increases the electric resistance and further impairs the tensile strength of the joint. The pores are divided into process pores ($r_{\text{pore}} \gg 0.1 \text{ mm}$), which are caused by capillary instabilities, and metallurgical pores ($r_{\text{pore}} < 0.1 \text{ mm}$), which are caused by changes in the solubility of substances in the copper melt. The influence of process parameters on the tensile strength was investigated by Dimatteo et al., 2021. Those previous studies consider the effects on pore formation and decrease of tensile strength separately. This work presents a holistic comparison of pore formation and the resulting tensile strength of the joined hair pins. In order to capture the effects during pore

and spatter formation the welding process was analyzed by means of highspeed imaging and online x-ray imaging.

2. Method

An X-ray tube is used for X-ray imaging of the processing zone during the weld process. The X-ray imaging system is described in detail by Abt et al., 2011; Abt et al., 2018; Boley et al., 2019 . The recorded images present a grey-scale distribution, which is defined by the local absorption of the X-rays according to beer's law. This allows to differentiate between the vapor capillary (bright, due to less absorption) and the solid material (dark, due to higher absorption). To reduce noise a flat-field correction is used, which is based on the subtraction of the image of two pins before welding from the process images during welding. This results in very bright areas around the welded pair of pins. The hairpin windings (Cu-ETP) are rectangular with 4 mmx1 mm. For all experiments, a disk laser TruDisk 8001 with a beam transporting fiber of $d_{TF}=100\ \mu\text{m}$ was used. Using a PFO 33, resulted in a beam waist of $d_f=170\ \mu\text{m}$ which was positioned on the surface of the pins for all experiments and moved the laser beam over the hairpins. The beam was moved over the pins several times until all corners of the pins were melted. For all the experiments a power ramp at the beginning of the weld was used. The power ramp started at 20% of the total power and reached 100 % of the laser power at the end of the first completion of the welding contour. The welding process was additionally recorded with a high-speed camera (8 kHz) to record the formation of spatters at the surface. The number of spatters was quantified by the sum of all images, which presents brightest value occurred during the process at each pixel.

Results

The formation of process pores was observed by means of X-ray imaging of the welding process. Fig 1. shows different time steps of a hairpin welding process from the side-view (left) and the corresponding X-ray image where the capillary geometry is highlighted in dashed white lines to guide the eye. As described in Omlor et al. the process pore formation was observed mostly when moving the laser beam over the gap. It was observed, that the movement of the laser beam over the gap is associated with an increased spatter formation (Fig. 1, 12.6 ms), melt ejection (Fig. 1, 17.3 ms) and pore formation (Fig. 1, 32 ms). It can be seen that during the laser beam passes the gap for the first time a melt ejection occurred (12.6 ms), which coincides with spatter formation. After the third pass (32 ms), the crater of the melt ejection is not visible anymore, but a process pore was formed. This process pore was equalized during the fourth overdrive. It results in a welded hairpin without process pores (bottom, right). To determine the influence of the welding contour on the pore formation, different contours with the same laser power are compared in Figure 2, which presents one representative welded hairpin for each welding contour. One can see that the welding contour influences the total amount of spatters and process pores occurred during the welding process.

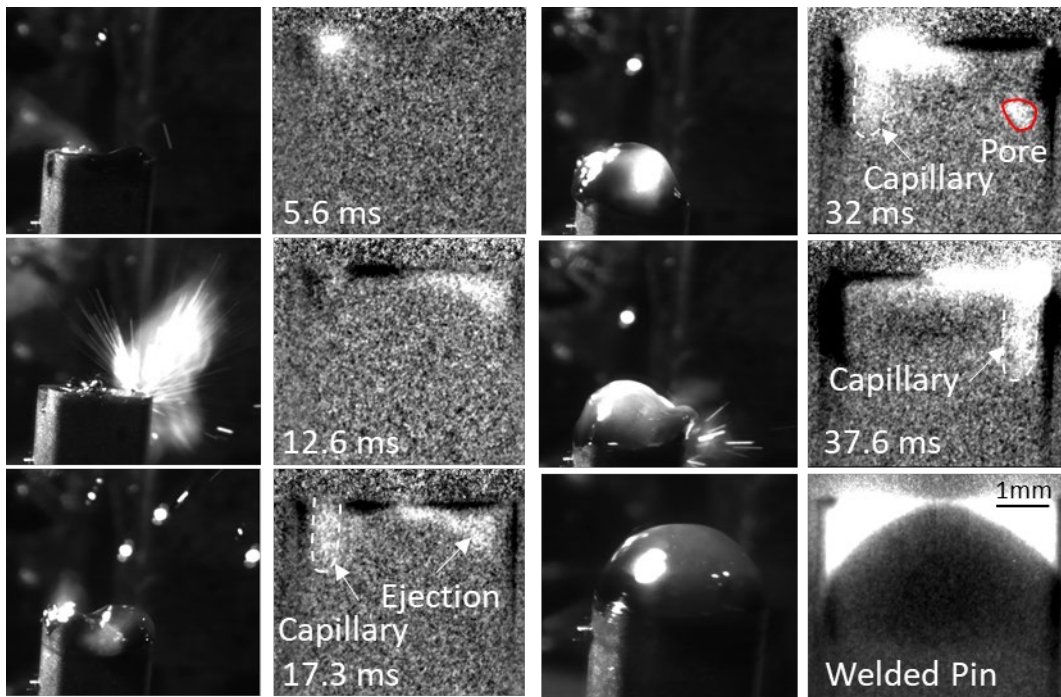


Fig. 1. Spatter (left images) and pore(X-ray images) formation due to melt ejection in previous overdrive (d_f : 170 μm , top-hat, 6kW; 600 mm^{-1})

The process pores are highlighted in red in the x-ray image of the welded hairpins in Fig. 2. The highest number of spatters occurred for the elliptical contour, while the lowest number of spatters occurred for the “8”- contour. It can also be seen that there is a difference in the total number of occurred spatters and process pores for the chosen welding direction of the spiral. Welding from the outside to the inside leads to less spatters and process pores than welding from the inside to the outside. It is assumed, that the heat accumulates in the center of the pin in case of welding a spiral from the outside to the inside. This preheating favors the avoidance of process pores in comparison to the weld with the spiral from the inside to the outside.

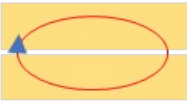
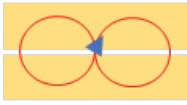

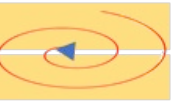


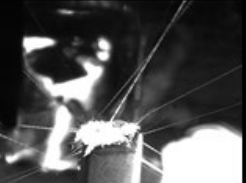

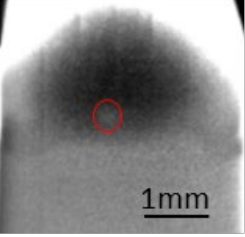
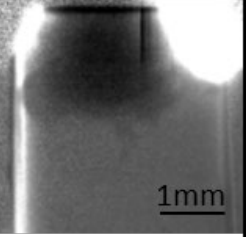
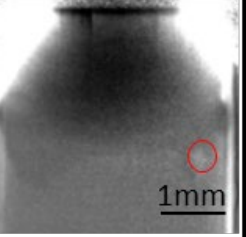
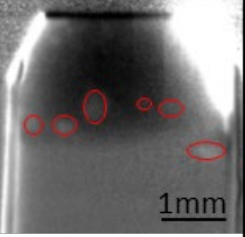
Welding Contour				
Sum-Image Spatters				
X-ray image welded Pins				
Parameter	$v = 600 \text{ mms}^{-1};$ $P = 6 \text{ KW}$	$v = 600 \text{ mms}^{-1};$ $P = 6 \text{ KW}$	$v = 500 \text{ mms}^{-1};$ $P = 6 \text{ KW}$	$v = 500 \text{ mms}^{-1};$ $P = 6 \text{ KW}$

Fig. 1. Different welding contours (top), the resulting spatter formation of the whole process and an X-ray image of the welded pins where process pores are visible.

The effect of the welding contour and chosen welding parameters on the max tensile force before fracture in case of a peeling load during tensile testing is shown in Figure 3. Three different welding parameters for the elliptical contour, resulting in three different process times and the “8” were chosen for a tensile test. For each parameter a representative fracture surface is shown. In the fracture surface the visible pores are highlighted by circles. The color of the circles indicates the size of the pore. Huge process pores are indicated in red and small metallurgical pores are highlighted in pink. In-between sized pores are highlighted in black.

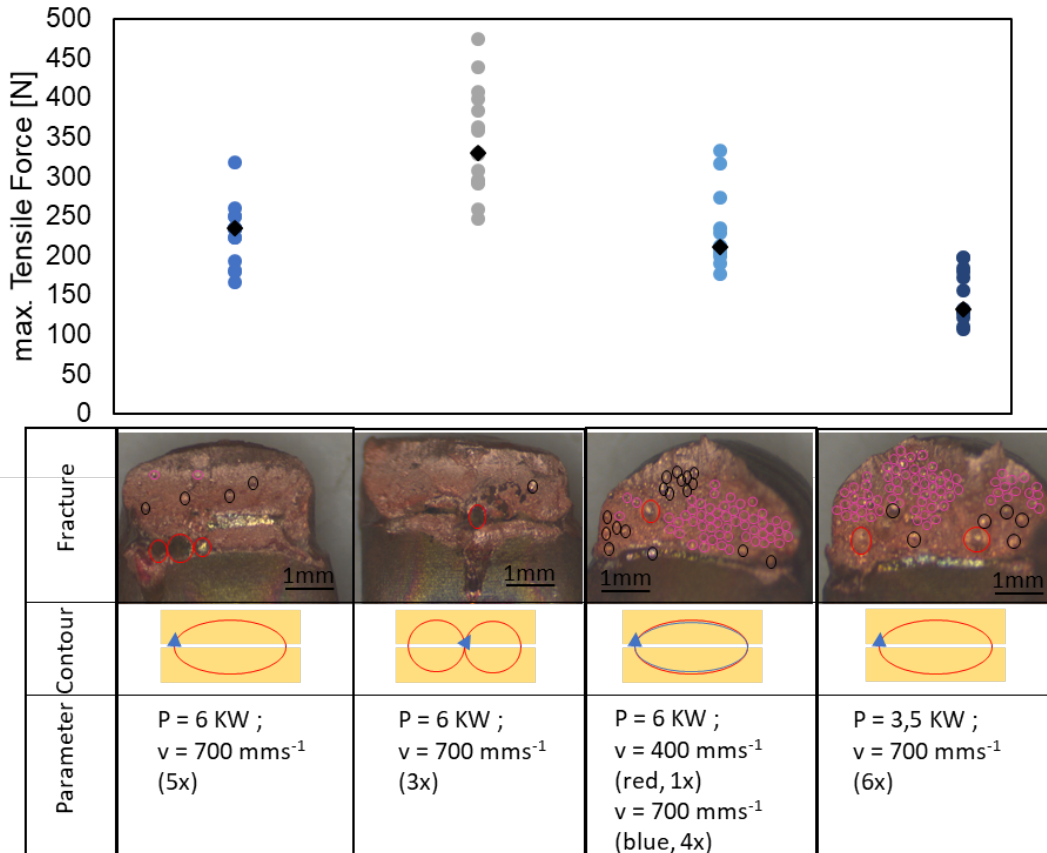


Fig. 2. Max tensile force for different welding contours and welding parameters resulting in different process times ($t_{proc} = 35$ ms (left); $t_{proc} = 38$ ms ("8"); $t_{proc} = 33$ ms (3rd); $t_{proc} = 70$ ms (right)).

One can see that although all pins are made out of the same Cu-ETP and all the pins are from the same batch, the amount of small metallurgical pores varies for the different welding contours. The most metallurgical pores are visible for the two samples with the longest process time in the right of Figure 3 with 132^{+56}_{-25} N. The weld with two different welding speeds has the shortest process time and shows the second lowest maximum occurred tensile force with 211^{+122}_{-34} N. The weld with the "8"-contour shows the lowest number of pores on the fracture surface and provides the highest tensile force of 330^{+144}_{-87} N. It can be seen that there is a high scattering on the max occurred tensile force, which probably results from strong deviations in pore formation. The comparison of the fracture surface with the tensile force indicates the direct connection between the number of pores and strength of the Weld.

3. Conclusion

The influence of different welding contours on the formation of process pores and spatters during welding hairpin windings was shown. The results show that both, the contour itself and its welding direction for the

spiral shows a significant influence on the formation of process pores and spatters. It indicates that in order to avoid pore formation a movement of the vapor capillary in preheated material is beneficial. Additionally, the welding strategy influences the number of metallurgical pores, which also influence the tensile strength of the weld. Further investigations are needed to determine the influence of the welding contour on the total number of pores. The results show clearly, that the generation of pores is directly connected with the gap. In order to avoid a passing of the laser at the gap new dynamic beam shaping strategies are required, eg. coherent beam combining. Future work will consider such strategies.

Acknowledgements

The research was funded in the framework of the industrial collective research programme (IGF no. 22.058N). It was supported by the Federal Ministry for Economic Affairs and Energy (BMWi) through the AiF (German Federation of Industrial Research Associations eV) based on a decision taken by the German Bundestag. The Laser beam source TruDisk8001 (DFG object number: 625617) was funded by the Deutsche Forschungsgemeinschaft (DFG, German Research Foundation) – INST 41/990-1 FUGG. The hairpin windings were provided by GROB-WERKE GmbH & Co. KG and the tensile test was performed by Gehrings Technologies GmbH & Co KG. The support of all funders and supporters is highly appreciated.

References

- Abt F., Boley M., Weber R., Graf T., Popko G., Nau S., 2011. Novel X-ray System for in-situ Diagnostics of Laser Based Processes – First Experimental Results. *Physics Procedia* 12, pp 761–770. doi: 10.1016/j.phpro.2011.03.095
- Abt F., Boley M., Weber R., Graf T., 2018. X-ray videography for investigation of capillary and melt pool dynamics in different materials. *International Congress on Applications of Lasers & Electro-Optics 2011*, pp 179–186. doi: 10.2351/1.5062233
- Alter L., Heider A., Bergmann J. P., 2020. Influence of hydrogen, oxygen, nitrogen, and water vapor on the formation of pores at welding of copper using laser light at 515 nm wavelength. *Journal of Laser Applications* 32, p 22020. doi: 10.2351/7.0000063
- Bocksrocker O., Speker N., Beranek M., Hesse T. Reduction of spatters and pores in laser welding of copper hairpins using two superimposed laser beams. In: *Laser in Manufacturing Conference*
- Boley M., Fetzner F., Weber R., Graf T., 2019. High-speed x-ray imaging system for the investigation of laser welding processes. *Journal of Laser Applications* 31, p 42004. doi: 10.2351/1.5110595
- Dimatteo V., Ascari A., Faverzani P., Poggio L., Fortunato A., 2021. The effect of process parameters on the morphology, mechanical strength and electrical resistance of CW laser-welded pure copper hairpins. *Journal of Manufacturing Processes* 62, pp 450–457. doi: 10.1016/j.jmapro.2020.12.018
- Glaessel T., Seefried J., Franke J., 2017. Challenges in the manufacturing of hairpin windings and application opportunities of infrared lasers for the contacting process. In: *2017 7th International Electric Drives Production Conference (EDPC)*. IEEE
- Heider A., 2018. Erweitern der Prozessgrenzen beim Laserstrahlschweißen von Kupfer mit Einschweißiefen zwischen 1 mm und 10 mm. *Dissertation, Universität Stuttgart*
- Heider A., Stritt P., Hess A., Weber R., Graf T., 2011. Process Stabilization at welding Copper by Laser Power Modulation. *Physics Procedia* 12, pp 81–87. doi: 10.1016/j.phpro.2011.03.011
- Omlor M., Reinheimer E. N., Butzmann T., Dilger K. Investigations on the formation of pores during laser beam welding of hairpin windings using a high-speed x-ray imaging system. Submitted to *Journal of Laser Applications* 01/2023